Investigation of pulse voltage shape effects on electrohydrodynamic jets using a vision measurement technique

2013 J. Micromech. Microeng. 23 065018

(http://iopscience.iop.org/0960-1317/23/6/065018)

J. Micromech. Microeng. **23** (2013) 065018 (12pp) doi:10.1088/0960-1317/23/6/065018

Investigation of pulse voltage shape effects on electrohydrodynamic jets using a vision measurement technique

Kye-Si Kwon[1] **and Dae-Yong Lee**

Department of Mechanical Engineering, Soonchunhyang University 646, Eupnae-ri, Shinchang-myeon, Asan-si Chungnam, 336-745, Korea

E-mail: kskwon@sch.ac.kr and http://inkjet.sch.ac.kr/

Received 23 November 2012, in final form 21 March 2013
Published 7 May 2013
Online at stacks.iop.org/JMM/23/065018

Abstract
In this paper, we present a vision measurement technique to evaluate electrohydrodynamic (EHD) inkjet behavior, and discuss the effects of the pulse voltage shape on the EHD jets for drop-on-demand printing, including the falling and rising time in the pulse voltage. Sequential images acquired by a charge-coupled device (CCD) camera with a strobe light-emitting diode (LED) were used to visualize EHD jet behavior with respect to time. A vision algorithm was implemented in an EHD jet system to enable *in situ* measurement and analysis of EHD jets. A guideline for selecting pulse shape parameters is also presented, to enable the achievement of high-frequency reliable jets for drop-on-demand printing. Printing results are presented to demonstrate the drop consistency of jets.

(Some figures may appear in colour only in the online journal)

1. Introduction

The application of inkjet technology has been broadening from home printers to manufacturing tools. Recently, a need emerged for high-resolution printing, especially in the field of printed electronics applications [1, 2]. However, the droplet volumes of 1–2 picoliters (pL) produced with nozzle diameters of 16 μm limit current inkjet technology [1]. As an alternative technique for fine printing, electrohydrodynamic (EHD) inkjet technology has recently been drawing attention, because it has advantages over the conventional inkjet pattern method, in that droplets smaller than the nozzle diameter can be ejected, and materials with a wider viscosity range could be used for jetting. Successful direct printing of a few microns of conductive lines in width has been reported using the technology [1–3].

To achieve fine patterning, the parameters affecting the EHD jet should be optimized, including ink conductivity, ink surface tension, nozzle diameter, driving voltage, flow rate (or air pressure) and stand-off distance between the nozzle and substrate [4]. Among these parameters, one of the easiest ways to change the jet behavior is to change the shape of the driving voltage. Electrostatic forces generated from high-voltage sources are used to eject charged droplets onto a substrate. The voltage driving schemes can be classified as (1) dc voltage only schemes [2], and (2) those involving pulse voltages superposed on a dc field [5–9]. In this study, pulsed voltage superposed with dc is mainly discussed, because it makes drop-on-demand printing easier. The dc background voltage is used to maintain the extruded meniscus under nonjetting conditions by balancing the forces of fluidic pressure, surface tension and electrostatic force.

To use EHD jets in drop-on-demand printing applications, each pulse voltage should produce a single droplet. To optimize the pulse voltage, it is important to understand the jet behavior in relation to the shape of the pulsed voltage. In particular, the jet start time needs to be understood with respect to the pulse voltage. The jet start time should remain the same irrespective of the jet frequency. Otherwise, jet placement error may occur, because the motion stages for the head or the substrate move during drop-on-demand printing. To evaluate pulse voltage in relation to jet behavior, proper measurement methods should be used. For jet evaluation, the printed patterns can be investigated [5, 11], or the jet behavior can be measured directly based on vision methods [7, 8, 12]. The method based

[1] Author to whom any correspondence should be addressed.

on printed patterns may not be a quick or easy approach, because it requires inspection of the printed patterns on a substrate. Moreover, it may be difficult to gain physical insight on the jet start time with respect to the pulse voltage. Therefore, vision-based measurement methods are more suitable for evaluating jetting performance. High-speed cameras [2, 11] and CCD cameras using LED strobe lights have been used for measurements [12, 13].

In this study, vision measurement and analysis techniques for pulsating EHD jets are mainly discussed. Since pulsating jets normally occur over a very short period of time (less than 100 μs), high frame rate is required to capture the jet behavior when using a high-speed camera. For proper analysis, a large amount of images must be recorded. As a result, real-time or *in situ* image analysis is difficult, since the acquired images are stored in the high-speed camera first and then downloaded to a computer for postprocessing. This process might require significant time and effort, so the use of high-speed cameras might be limited to cases when jet behavior during short periods needs to be analyzed (less than a few seconds). However, the first few droplets might be more dependent on ink drying characteristics on the nozzle surface rather than the pulse driving voltage. It is important to measure the steady-state jet performance if the effects of the driving pulse on an EHD jet are to be investigated. As such, high-speed cameras might not be suitable to evaluate pulse shape effects on EHD jets. High-speed cameras are also prohibitively expensive for use in manufacturing systems to monitor jet behaviors.

Alternatively, CCD cameras with strobe LEDs have widely been used to measure jet behavior in conventional inkjet heads [13]. In this work, the application of strobe LEDs is extended to EHD jet measurement. Sequential images using strobe LEDs are acquired to characterize the EHD jet behavior in relation to the pulse voltage.

The information extracted from EHD jet images should differ from that obtained with conventional inkjet images, because the jet behavior and drop formation of EHD jets are quite different. For example, pulsating jets with short duration might occur rather than a single spherical droplet per pulse voltage. To understand the jet behavior, we analyze the meniscus height with respect to time rather than the pulsating jet (or jetted droplet) in flight. For this purpose, we developed software capable of extracting the meniscus profile under jetting conditions. The main advantage of the proposed scheme is that *in situ* meniscus measurement enables quick and easy understanding of the jet phenomena in relation to the pulse voltage. As a result, the experimental conditions for DOD printing can be determined without carrying out actual printing experiments.

The effects of the voltage pulse width and amplitude on the EHD jet have been investigated in previous studies [8, 11, 12]. However, it seems that general guidelines for determining pulse voltage parameters have not yet been established. Also, few published studies discuss the effects of pulse shape on EHD jets, including the rising and falling parts of the pulse. In this study, we investigate these effects based on the meniscus behavior measured in vision analysis. We found that the rising, falling and dwell parts of the pulse voltage affected the EHD jet in different ways. By changing the pulse shape, the jet starting time and jet duration can be adjusted. To verify the jet consistency, drop-on-demand printing results are presented.

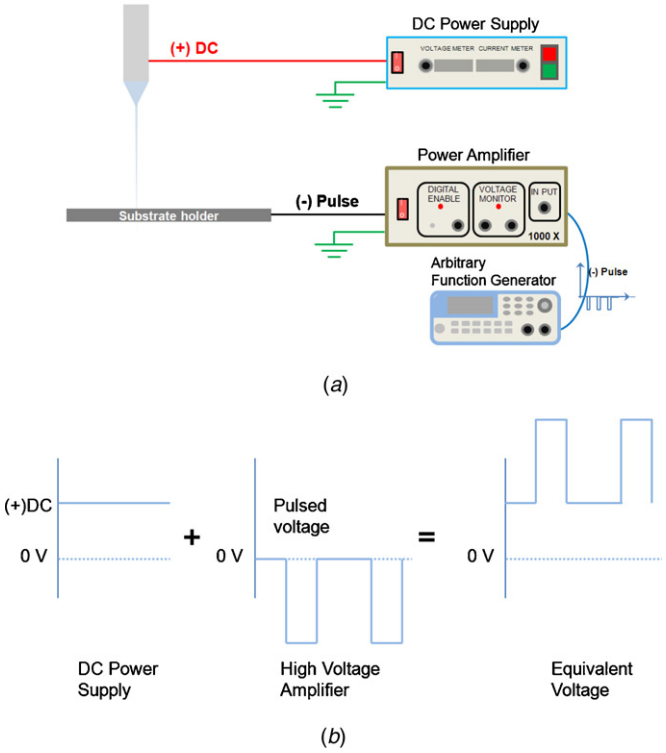

Figure 1. A voltage driving scheme for electrohydrodynamic (EHD) jets. (*a*) Voltage driving schemes using two voltage sources. (*b*) Equivalent driving voltage.

2. A vision measurement technique for EHD jets

2.1. EHD jet measurement system

EHD jet behaviors can differ according to the jet system configuration. For fluidic systems, constant flow rate using a syringe pump or constant pressure control using the pneumatic or fluid height can be considered. To apply electrostatic force to eject droplets, either a constant dc voltage or a pulse voltage with dc background can be considered.

In this study, the ink meniscus at the nozzle is maintained by means of hydrostatic pressure, which is adjusted by the height level difference between the nozzle and the ink reservoir. The ink reservoir is placed slightly higher than the nozzle to maintain an extruded meniscus. A constant flow rate using a syringe pump may not be suitable for drop-on-demand printing. The jet performance can be significantly affected by the jet frequency due to the constant flow rate of fluid from a syringe pump [5, 11].

A pulse voltage with dc background is used in this study, since the pulse voltage can be used effectively in drop-on-demand printing. For this purpose, two different high-voltage sources were used to obtain the pulse voltage with dc background, as shown in figure 1. A dc power supply was used for the background voltage, and a high-voltage amplifier was

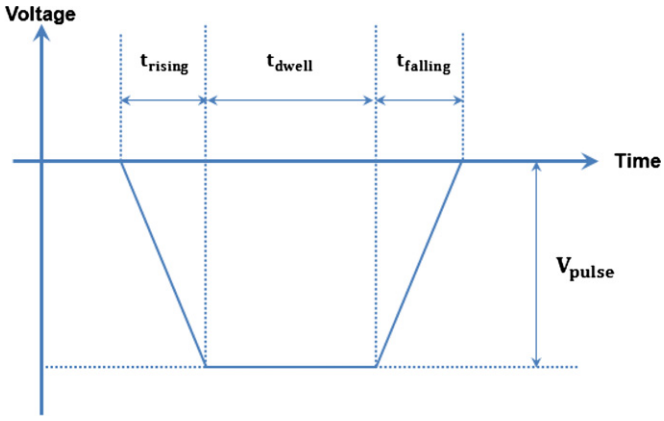

Figure 2. Driving pulse voltage.

used for pulsed voltage. A background dc voltage (or pulse voltage) is applied at the nozzle, whereas a pulsed voltage (or dc voltage) is applied at the substrate holder. If the dc background voltage is positive, the pulsed voltage should be negative, and vice-versa. As shown in figure 1(*b*), the driving voltage can be equivalent to that of a single power amplifier, which amplifies both V_{dc} and V_{pulse}. The use of two different high-voltage sources has advantages in that the maximum voltage requirement for the high-voltage amplifier can be reduced. The reduction of the maximum voltage requirement for the power amplifier is important, because it can potentially address many practical issues such as cost, the heat generated from the power amplifier and implementation in multinozzle systems. Dc power supplies for high voltage are cheap, and there are no practical issues.

A simple trapezoidal pulse was considered as the driving pulse voltage, as shown in figure 2. The pulse voltage data are generated by a computer and uploaded via serial communication to an arbitrary function generator (33220A, Agilent, USA). The pulse voltage data are stored in the memory of the function generator while waiting for the trigger pulse to generate the pulse voltage. Then, a high-voltage power amplifier (609E-6, TREK, USA) is used to amplify the pulse voltage by a factor of 1000. A high-voltage dc power

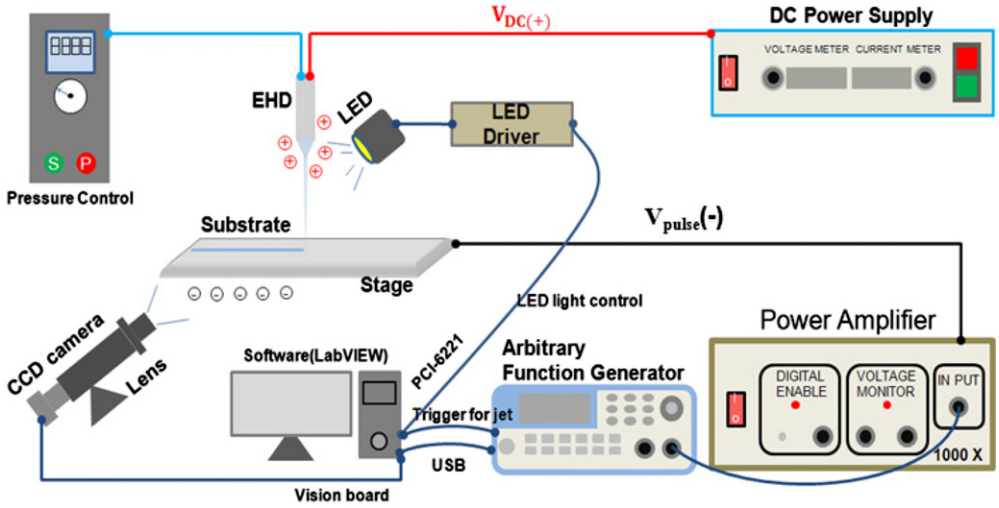

(*a*)

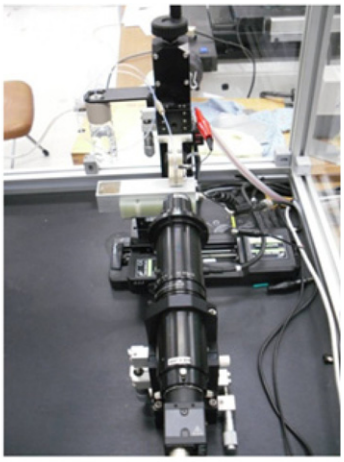

(*b*)

Figure 3. An EHD jet system. (*a*) Schematic of the EHD jet system. (*b*) Photo of the EHD jet system.

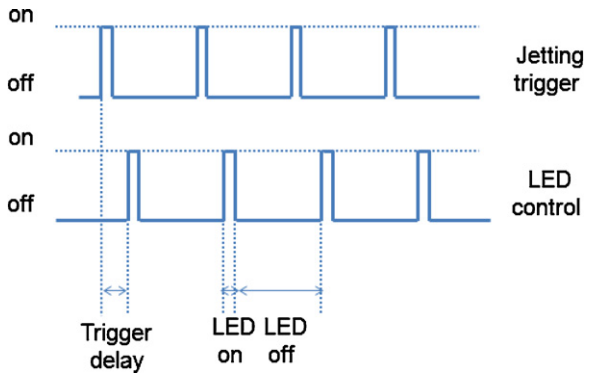

Figure 4. Strobe LED control.

supply (SHV 5 kV, Convertech, Korea) was used for the dc background voltage.

Figure 3 shows a schematic and photo of the EHD jet system developed for the visualization of jet images and for printing. To visualize the jet images, LED lights were synchronized with respect to jet triggers. Two digital pulse trains from a counter board (PCI-6221, NI, USA) are used for the synchronization, as shown in figure 4. The first digital pulse train is used as a trigger signal to generate the pulse voltage. The second pulse train is used to control the LED light. The second pulse is triggered from the first pulse. The trigger delay time between the first pulse and second pulse is adjusted such that the jet image at the delayed time can appear to be frozen in the acquired image.

A CCD camera (XC ES 50, Sony, Japan) was used for jet image acquisition. An adjustable zoom lens (ML-Z07545, MORITEX, Japan) and a lens adaptor (ML-Z20, MORITEX, Japan) were used to acquire magnified images of the EHD jet behavior. To obtain sufficient strobe light for visual measurement, a 5 W LED was used.

Standard inkjet ink (XL-30, Dimatix, USA) was used as a jetting fluid. For jet consistency, the fluid characteristics, such as the ink viscosity, need to be consistent during the experiments. To maintain constant ink viscosity, a heater is placed on the EHD head to maintain the temperature of the fluid at 30°. The viscosity of the ink is about 11 centipoise (cP) at 30 °C. For the experiment, a nozzle with an inner diameter of 50 μm was used.

2.2. *Image analysis*

The following pulse voltage parameters are used for an EHD jet to explain the image analysis algorithm: $t_{\text{dwell}} = 300$ μs, $V_{\text{pulse}} = 1500$ V, $V_{\text{dc}} = 500$ V, $t_{\text{rising}} = 0$ and $t_{\text{falling}} = 0$, $f = 500$ Hz and $g = 300$ μm. These parameters are the dwell time, the amplitude of the pulse voltage, the amplitude of the dc voltage, the rising time, falling time, jet frequency and stand-off distance between the nozzle and the substrate, respectively.

Figure 5 shows a selected sequential images of an EHD jet measured using the strobe LED. As shown in figure 5(*d*), a pulsating EHD jet is observed at 325 μs after the jet trigger signal. The EHD inkjet drop formation is quite different from that of a conventional inkjet printhead. As shown in figure 5(*d*), the pulsating jet is difficult to analyze, because the shape of the jet is thin and very long, so we analyze the extracted meniscus profile rather than directly analyzing the jet in flight, unlike conventional inkjet measurement.

Figure 6 shows the image processing algorithm to extract the meniscus profile. First, the image is converted to a binary image, since the jet shape in the binary image shape can be modified easily. Morphology functions from an NI vision development module (National Instruments, USA) are used for this purpose. For example, the thin, long part of the jet can be removed easily from the morphology process. Then, an ROI (region of interest) is defined around the meniscus to specify the image analysis area. In the two-dimensional ROI, predetermined horizontal-line ROIs are defined to detect edges, which have information about the meniscus profile. The detected edge locations were saved as a file for further processing of the extracted meniscus profile.

The extracted meniscus profiles can be shown in a 3D graph to investigate the meniscus behavior with respect to time. The time interval between consecutive sequential images can be selected in our software. For example, a time interval of

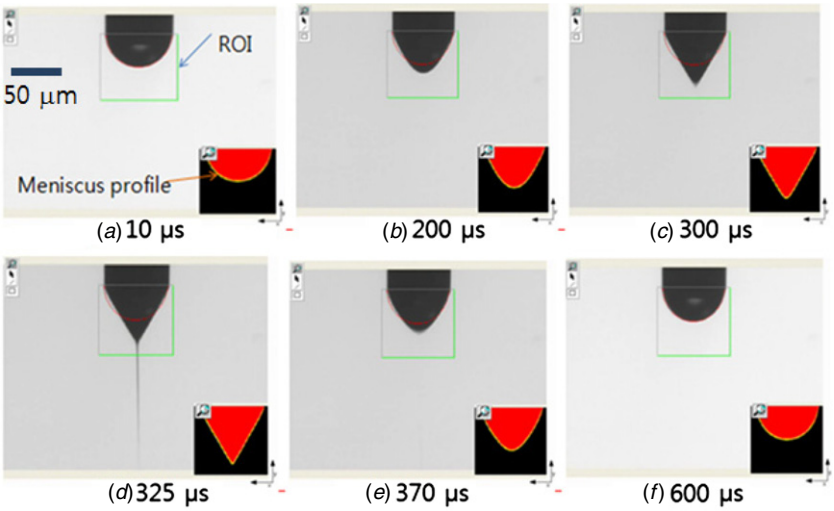

Figure 5. Typical EHD jet images ($V_{\text{dc}} = 500$ V, $V_{\text{pulse}} = 1500$ V, $t_{\text{rising}} = 0$, $t_{\text{falling}} = 0$, $t_{\text{dwell}} = 300$ μs).

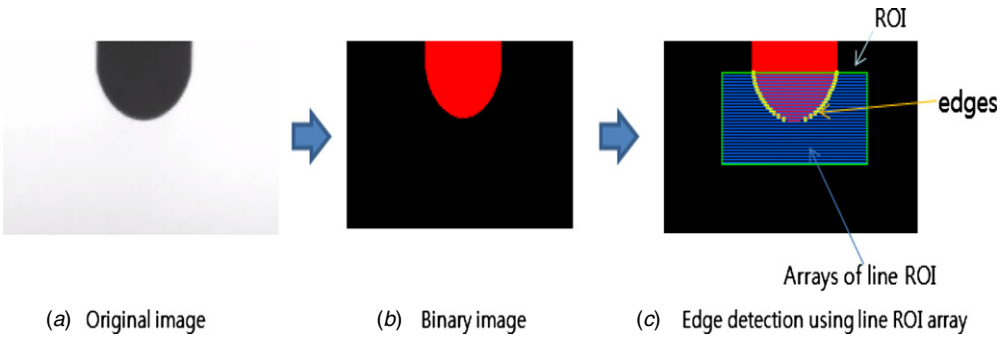

Figure 6. Image processing algorithm for extracting the meniscus profile.

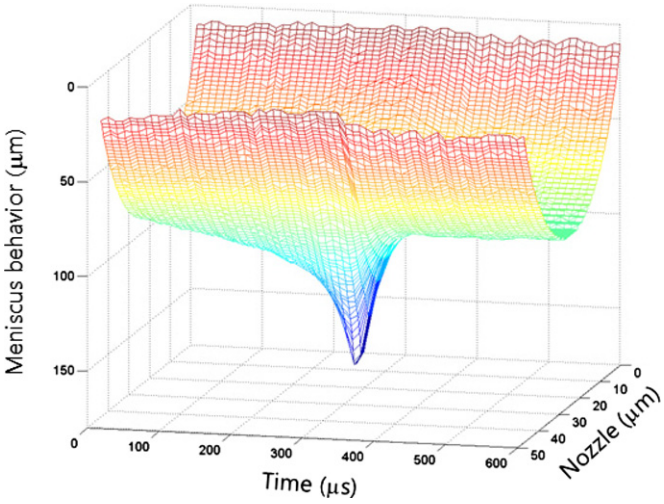

Figure 7. 3D graph of meniscus profiles [14].

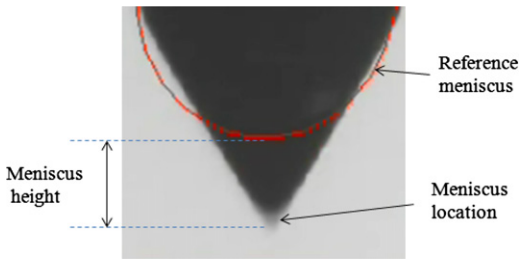

Figure 8. Meniscus height.

10 μs was selected in this study to analyze the jet behavior. Figure 7 shows a 3D graph of meniscus profiles when a time interval of 10 μs is used to acquire and analyze sequential images via the strobe LED.

The jet behavior was characterized by the meniscus height. The meniscus height used to evaluate the EHD jet is defined by the difference between a reference and the monitored maximum location of the meniscus profile in the downward direction, as shown in figure 8. The jet behavior of an EHD jet can be understood by the meniscus height variation with respect to time.

When a pulsed voltage is applied, the meniscus height increases to produce a jet. After jetting, the meniscus should be returned to the reference position to produce a consistent and repeatable jet at the next pulse voltage. Figure 9(*a*) shows the measured meniscus behavior during an EHD jet. A video is available online for better understanding of our measurement scheme [14]. An EHD jet is likely to occur when the meniscus height reaches close to a peak (around 310 μs), as shown in figure 9(*a*). It may be easier to explain the jet process if the meniscus velocity is used in relation to the meniscus behavior. The EHD jet process can be divided into three regions: (1) the initial meniscus deformation (1–300 μs); (2) jet (300–350 μs); and (3) relaxation (350–500 μs). During the initial meniscus deformation, the meniscus height gradually moves downward. The time length of the initial meniscus deformation was the same as the dwell time. When the falling part of the voltage was applied at 300 μs, the maximum value of the meniscus speed was observed, and the pulsating jet started. During the pulsating jet (300–350 μs), the meniscus speed decreases from positive to negative. The speed of the meniscus becomes zero at 310 μs when the maximum meniscus height is obtained. After 310 μs, the speed becomes negative, which means that the meniscus height changes its direction to upward. The pulsating jet is no longer observed after 350 μs. During the relaxation time (350–500 μs), the meniscus returns to the reference position without a jet until the speed becomes zero at 500 μs. The whole jet process ends at 500 μs. No jet is observed at this time, and the meniscus height becomes equal to the reference height. This means that the maximum jet frequency could be increased up to 2 kHz. The maximum jet frequency from the EHD inkjet head is related to the nozzle diameter, and it can be increased further if a smaller nozzle diameter is used [10]. However, the high jet frequency will affect the jet behavior, because the equivalent dc background voltage increases accordingly. This will be discussed later in detail.

To understand the jet behavior of different ink, nano silver ink (IJ-060, Inktec, Korea) was used for comparison. At 30° C, the viscosity of nano silver is 10 cp, and the surface tension is 35 mN m^{-1}. The amplitude voltage was adjusted to obtain the proper jetting of the nano silver ink. Voltages of $V_{\text{pulse}} =$ 500 V and $V_{\text{dc}} =$ 350 V were used for jetting. The rising, dwell and falling times for the pulse were set to $t_{\text{rising}} = 0$ μs, $t_{\text{dwell}} =$ 300 μs and $t_{\text{falling}} = 0$ μs, respectively. Then, the measured meniscus behavior of the nano silver ink (dotted line) was compared with that of the standard ink, as shown in figure 9. The jet start time and relation time were similar, because they are related to the pulse voltage rather than the properties of the ink. However, the response at the initial stage, the maximum meniscus location and the speed of the meniscus

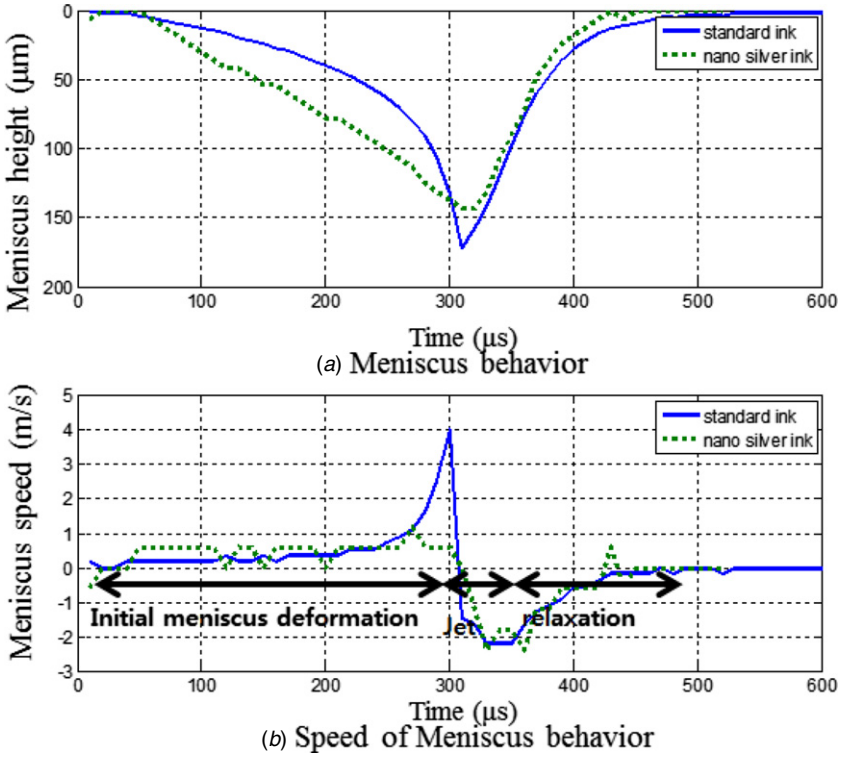

Figure 9. Meniscus height and speed.

behavior differ, because these parameters are related to the ink properties, such as the elasticity and conductivity. For example, nano silver ink a faster response at the initial stages (0–300 μs), but the jet occurs at a lower meniscus location with less meniscus speed at the time of the jet than with standard ink. Even though the jet behaviors of the initial stage (0–300 μs) were different, the jet and relaxation behaviors of the two different inks were similar.

As shown in figure 9, both the meniscus height and meniscus speed can be effectively used to explain EHD jet behavior. However, in this study, the meniscus height behavior is mainly used to explain the pulse effect on EHD jets, because it enables the overall jet behavior to be understood at a glance.

It has been reported that the pulse voltage creates shear (or tangential) stress rather than normal stress. The shear stress could result in a cone-shaped pulsating jet rather than spherically shaped droplets [7, 8]. This pulsating jet might negatively affect placement accuracy compared to a single spherical droplet per jet trigger signal. However, the pulsating jet is not likely to cause significant placement errors unless the printing speed is high. We can calculate the maximum printing speed, V_m, from the maximum jet frequency, f_m, and the drop spacing, d_s, as

$$V_m = d_s * f_m. \quad (1)$$

If a maximum jet frequency of 2 kHz and a drop spacing of 10 μm are used for printing, the maximum printing speed will be 20 mm s^{-1}. If the maximum printing speed is given, the possible jet placement error, E, can be calculated from the printing speed and jet duration, $t_{duration}$, as

$$E = V_m * t_{duration}. \quad (2)$$

If the jet duration and printing speed are assumed to be 50 μs and 20 mm s^{-1}, respectively, the possible placement error will be 1 μm. To reduce the drop placement error, either the printing speed or jet duration should be reduced.

The jet behaviors can be understood from the proposed *in situ* and automatic vision measurement, and the efforts for optimizing jet conditions can be reduced significantly. For reliable measurement using the strobe LED, the jet behavior should be consistent, and the same behavior should be repeated at each pulsed voltage. If the jet behavior from each pulse voltage is not consistent, there will be significant blur in the images.

3. Pulsed voltage effects on EHD jet

3.1. Dwell time effects

To obtain stable EHD jets, the voltage amplitudes, V_{pulse} and V_{dc}, should be selected appropriately. If V_{dc} increases, V_{pulse} can be decreased for the jet [7, 8, 12]. However, to use EHD jets in drop-on-demand printing applications, it is recommended that the amplitude of V_{pulse} be larger than that of V_{dc} to ensure a single pulsating jet per pulse voltage. However, if V_{pulse} is too large, problems with frequency dependence on the EHD jet and high-voltage requirements for the amplifier arise. By considering the trade-off relationship, we recommend that the amplitude of V_{pulse} be set to 1.2–3 times higher than that of V_{dc}.

The effect of the pulse width on the EHD jet has been discussed in previous works [7, 8, 12]. In this section, the effects of dwell time on the jet start time and jet frequency are mainly discussed, based on meniscus behaviors measured by

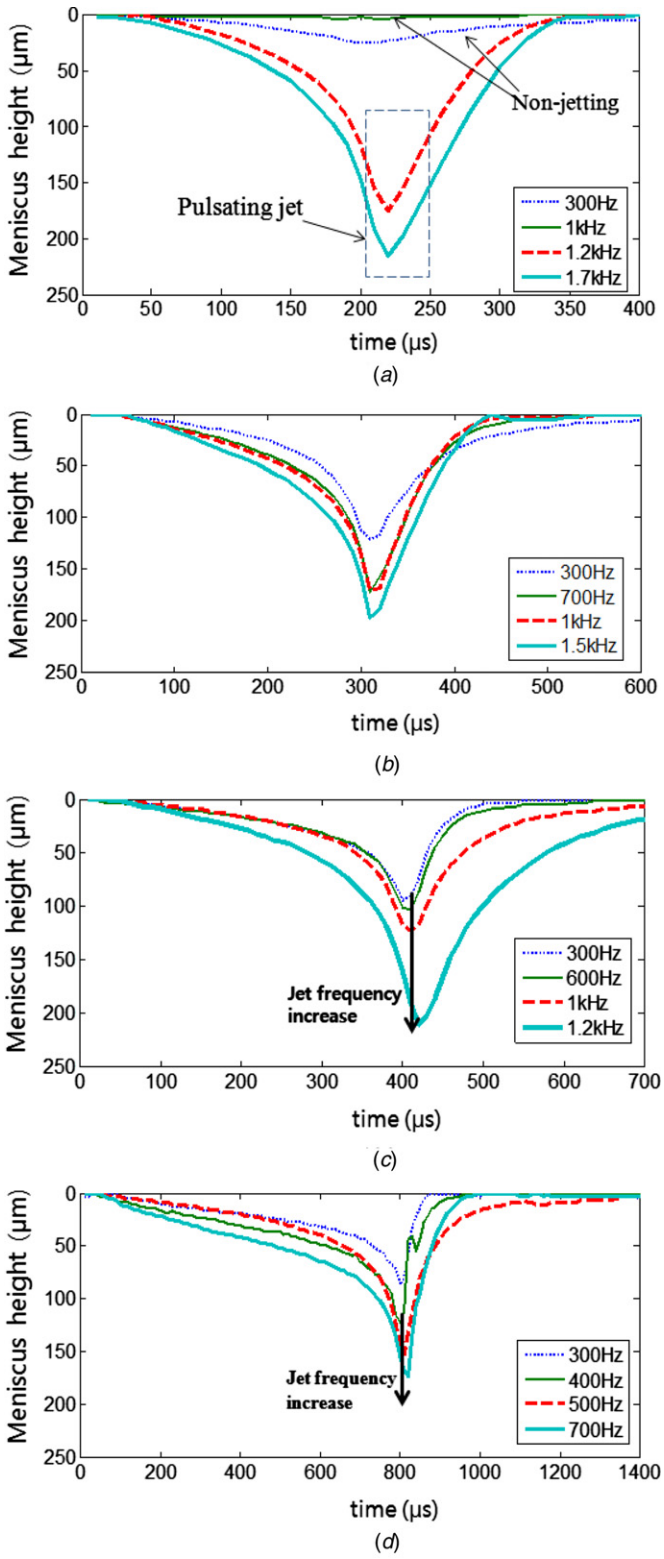

Figure 10. Dwell time effects on EHD jet ($V_{pulse} = 1500$ V, $V_{dc} = 500$ V, $t_{rising} = 0$, $t_{falling} = 0$). (*a*) $t_{dwell} = 200$ μs, (*b*) $t_{dwell} = 300$ μs, (*c*) $t_{dwell} = 400$ μs, (*d*) $t_{dwell} = 800$ μs, (*e*) $t_{dwell} = 900$ μs, (*f*) $t_{dwell} = 1000$ μs.

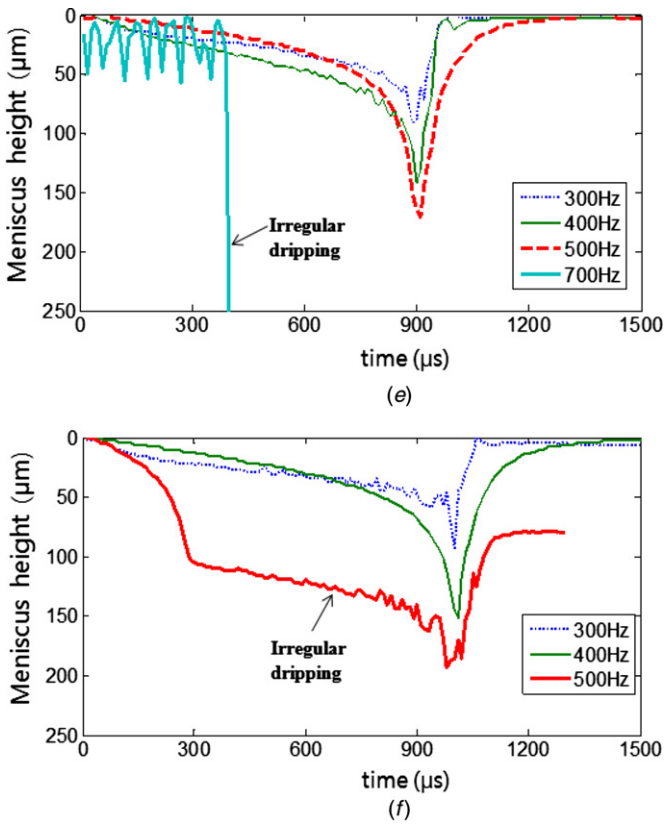

Figure 10. (Continued.)

our vision system. For this purpose, the fixed amplitudes of $V_{dc} = 500$ V and $V_{pulse} = 1500$ V are used. Figure 10 shows the meniscus behavior according to dwell time and jet frequency. The meniscus behavior was measured with respect to time using the proposed vision analysis methods.

There is a range of dwell times to obtain stable pulsating EHD jets. For example, drop-on-demand jets are not possible if a dwell time of less than 100 μs is used in our experiment. The minimum dwell time for the jet should be longer than 200 μs, because the meniscus needs to be sufficiently pulled down to the substrate before it becomes a pulsating jet. On the other hand, if the dwell time is longer than 1000 μs, irregular dripping is observed during the pulsed voltage. This irregular dripping cannot be used in printing applications. In some cases, it has been reported that more than one droplet could be observed if a long period of pulsed voltage is used [6].

To maximize the jet frequency, the shortest possible dwell time is recommended, because shorter dwell time can result in shorter time for the meniscus to return to the reference position. Based on the experimental results shown in figure 10, the dwell time of 300 μs is recommended for a wider range of EHD jet frequency. For example, for a 300 μs dwell time, the meniscus returns to the reference position at approximately 500 μs, as shown in figure 10(*b*). However, for a 900 μs dwell time, the required time could be more than 1000 μs. When the meniscus returns to the reference position after a jet, the next pulse voltage can be applied for the next jet. However, the jet behavior could be affected by the jet frequency, because the jet frequency influences the equivalent dc background voltage. The equivalent dc voltage, $V_{dcequiv}$, can be calculated as

$$V_{dcequiv} = V_{dc} + V_{pulse} * t_{dwell} * f. \quad (3)$$

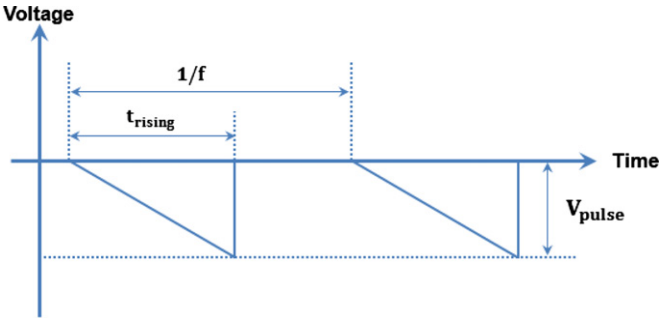

Figure 11. Pulse voltage with rising time only.

The equivalent dc voltage, V_{dcequiv}, might increase significantly from V_{dc} if the dwell time, t_{dwell}, is long, and the jet frequency, f, becomes high. The meniscus height prior to the EHD jet becomes higher when the jet frequency increases, as shown in figures 10(*c*) and (*d*), because of the larger equivalent dc voltage. As a result, the amount of jet might also be affected. If the dc effect becomes large and dominant, large irregular droplets are likely to be observed. Irregular ink drippings were observed when $t_{\text{dwell}} = 900$ μs with $f = 700$ Hz or $t_{\text{dwell}} = 1000$ μs with $f = 500$ Hz was used for EHD jets, as shown in figures 10(*e*) and (*f*). To obtain uniform printing results, it is recommended that the operation conditions be selected such that the pulse voltage could be larger than the equivalent dc voltage, i.e. $V_{\text{pulse}} > V_{\text{dcequiv}}$. If the equivalent of dc voltage is low, there will be no jetting with low jet frequencies of 300 Hz and 1 kHz using $t_{\text{dwell}} = 200$ μs, as shown in figure 10(*a*).

The EHD jet is normally initiated at the time of maximum meniscus height. As shown in figure 10, the jet starting time, t_{start}, is almost the same as the dwell time, i.e. $t_{\text{start}} \approx t_{\text{dwell}}$. This means that the jet starting time can be controlled easily through the dwell time. As shown in figure 10, the jet start time of a dwell time remains the same, even when the jet frequency varies. These results are useful for printing in terms of minimizing the placement errors, since the jet frequency might vary due to the complexity of patterns to be printed. However, the amount of jet is likely to be larger when the jet frequency increases, because of the higher equivalent dc voltage. As discussed before, the time required for initial meniscus deformation prior to a jet is proportional to the dwell time. However, the required time for relaxation after a jet is likely to be similar, regardless of dwell time, as shown in figure 10.

3.2. Rising time effect on EHD jet

3.2.1. Rising time effect with $t_{dwell} = 0$. In this section, the effects of the rising time of the pulse voltage on EHD jets are investigated. As an extreme case, the dwell time of the pulse voltage is set to zero ($t_{\text{dwell}} = 0$), and only the rising time is varied. In this particular case, the total length of time of the pulsed voltage is equal to the rising time, as shown in figure 11.

Figure 12 shows the meniscus behavior according to rising time. As shown in figure 12, the rising time (t_{rising}) for stable EHD pulsating jets could be longer than the pulse voltage with dwell time. This is because the equivalent dc voltage of the pulse voltage in figure 11 can be lower than that of the

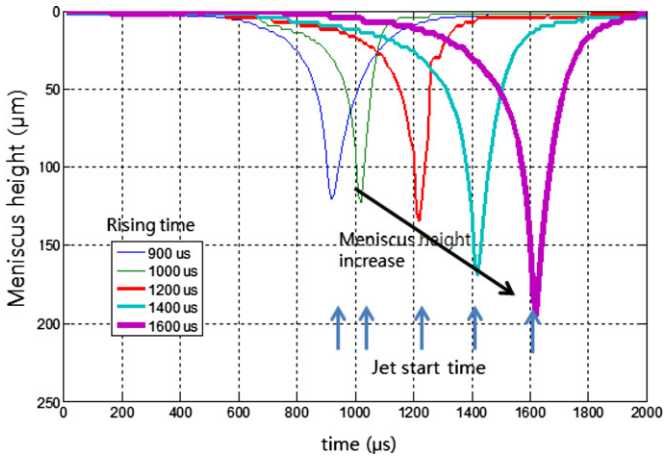

Figure 12. Rising time effects on meniscus behavior ($t_{\text{falling}} = 0$, $t_{\text{dwell}} = 0$, $V_{\text{pulse}} = 1500$ V, $V_{\text{dc}} = 500$ V, $f = 300$ Hz).

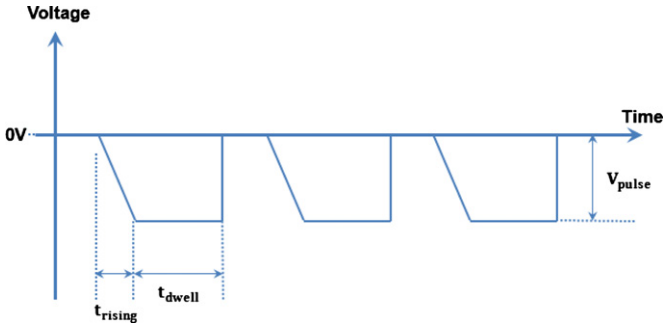

Figure 13. Pulsed voltage with rising time and dwell time.

pulse voltage with dwell time only if the total length of time is the same. The equivalent dc voltage of the pulse voltage in figure 11 can be written as

$$V_{\text{dcequiv}} = V_{\text{dc}} + 0.5 * V_{\text{pulse}} * t_{\text{risng}} * f. \tag{4}$$

Similarly to the case of using dwell time only, the jet start time is equal to the length of the pulse voltage. However, as the rising time lengthens, the meniscus maximum height prior to a jet increases, as shown in figure 12. There are two possible reasons for the increase in meniscus maximum height prior to a jet: that the equivalent dc voltage increases when a long rising time is used; and that the time for pulling down the meniscus increases due to the long rising time.

During the rising part of the pulse, the initial meniscus deformation can be more gradual due to the gradual increase in the pulse voltage. However, the maximum jet frequency is low compared to that of a simple pulse voltage, because the pulse length for a stable EHD jet is longer than when using a simple pulse voltage with dwell time only.

3.2.2. Rising time effect with $t_{dwell} \neq 0$ on EHD jet. In this section, to investigate the effect of rising time on EHD jet behavior, the pulsed voltage shown in figure 13 is considered. Rising times of $t_{\text{rising}} = 100$ μs, 200 μs and 400 μs were used, and the other parameters were set to fixed values of $t_{\text{falling}} = 0$ μs, $t_{\text{dwell}} = 400$ μs, $V_{\text{pulse}} = 1500$ V, $V_{\text{dc}} = 500$ V and $f = 500$ Hz. To investigate the jet consistency, the same

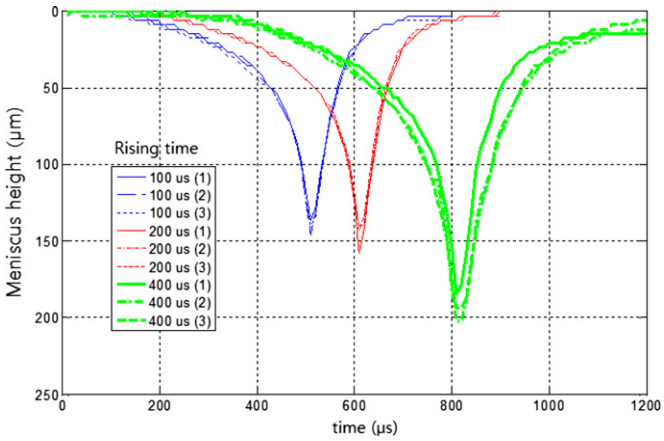

Figure 14. Rising time effects on meniscus behavior with dwell time ($t_{falling} = 0$ μs, $t_{dwell} = 400$ μs, $V_{pulse} = 1500$ V, $V_{dc} = 500$ V, $f = 500$ Hz).

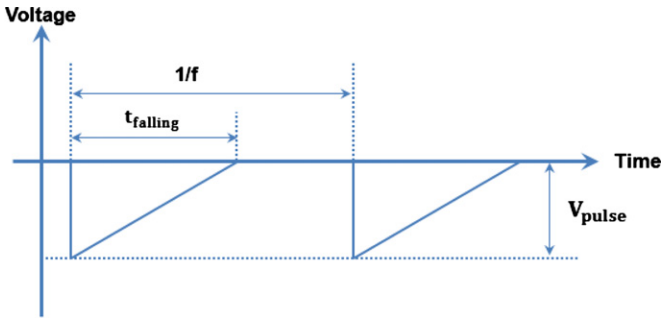

Figure 15. Pulsed voltage with various falling time ($V_{pulse} = 1500$, $V_{dc} = 500$ V, $t_{rising} = 0$ and $t_{dwell} = 0$).

measurements were repeated three times for comparison, as shown in figure 14.

As shown in figure 14, the jet starting time, t_{start}, is almost the same as the total length of a pulse:

$$t_{start} \approx t_{rising} + t_{dwell}. \quad (5)$$

As discussed in the previous section, there may be an advantage in using the rising time, in that the meniscus behavior can be stable due to the gradual change in the meniscus location to the jet location. However, the total time required for a pulse voltage is longer than that of a simple pulse voltage using dwell time only, which might limit the maximum jet frequency

3.3. Falling time effect for EHD jet

3.3.1. Falling time effect with $t_{dwell} = 0$ and $t_{rising} = 0$. To investigate the effect of falling time, the pulse voltage shown in figure 15 is investigated. In this experiment, the rising and dwell times were set to zero. Falling times between 200 and 1500 μs were selected to see if any stable EHD jets exist. However, no stable pulsating jet was observed if the pulse voltage shown in figure 15 was used. The reason for this is that the falling time is related to the jet rather than the initial meniscus deformation. The initial meniscus deformation is needed for the meniscus to be pulled down sufficiently prior to a jet, so before applying the falling part of the pulse, proper rising and falling times are required.

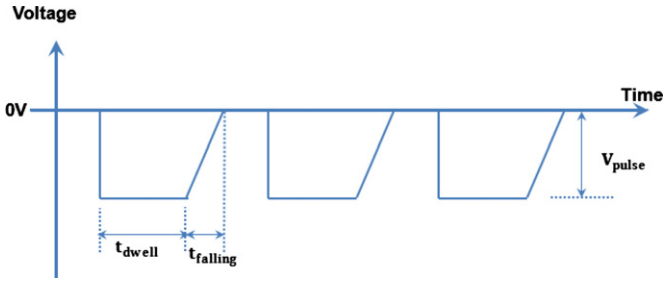

Figure 16. Pulse voltage with $t_{rising} = 0$, $t_{dwell} \neq 0$ and $t_{falling} \neq 0$.

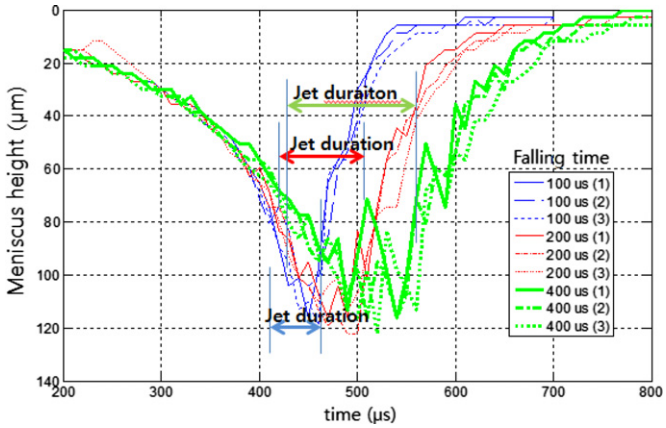

Figure 17. Falling time effects on meniscus behavior ($t_{dwell} = 400$ μs, $t_{rising} = 0$, $V_{pulse} = 1500$ V, $V_{dc} = 500$ V, $f = 500$ Hz).

The charge density, characterized by the product of voltage amplitude and duration, has been believed to account for the EHD jet [11]. However, in contrast, different jet behavior was observed, depending on the length of rising and falling time of the pulse voltage, even though the product of the pulsed voltage and the pulse duration was the same.

3.3.2. Falling time effect on jet with $t_{dwell} \neq 0$. To investigate the effect of the falling time on EHD jets, the pulse voltage shape shown in figure 16 was examined. The falling times of $t_{falling} = 100$, 200 and 400 μs were used, and the other parameters were fixed at $V_{pulse} = 1500$ V, $V_{dc} = 500$ V, $t_{dwell} = 400$ μs, $t_{rising} = 0$ μs and $f = 500$ Hz.

To investigate the jet consistency, the experiments were repeated three times for each falling time, as shown in figure 17.

As shown in figure 17, the jet behavior effect of the falling time differed significantly from those of the other voltage parameters. In the previous section, it was found that the jet start time is related to the total length of the pulse in the case of $t_{falling} = 0$ μs, as in equation (5). However, the jet start time might not correspond to the total length of time if the falling time is not zero. From the experimental results, we observed that the jet start time, t_{start}, can be written as

$$t_{start} = t_{rising} + t_{dwell} + t_d \quad (6)$$

where the time delay due to the falling time, t_d, is in the range of 20–50 μs. As shown in equation (6), the jet start time is mainly related to the rising time and dwell time, and less affected by

the jet delay due to the falling time. The delay time t_d was relatively shorter than the falling time, $t_{falling}$.

We observed in the experimental results in figure 17 that the jet duration could be increased by using a longer falling time. For example, with a falling time of 400 μs, the jet duration was increased to 150 μs. The jet duration could be less than 50 μs with zero falling time. In this way, the amount of jet can be adjusted by changing the jet duration. However, precise control of the jet duration could be difficult. In addition, as shown in figure 17, the meniscus behaviors of each EHD jet become less consistent if the falling time increases. This could result in variation in the jet amount.

The long falling time results in an increase in the equivalent dc voltage. However, even though the equivalent dc voltage might increase by using a loner falling time, the maximum meniscus heights were almost the same, regardless of the length of falling times, as shown in figure 17. This behavior is different from the effects of other pulse parameters such as dwell time and rising time. The maximum meniscus height was affected when these parameters changed the equivalent dc voltage, as discussed in previous sections.

If long falling time is used, EHD jets could end prior to the end of the pulse voltage. For example, with $t_{falling} =$ 400 μs, the total length of the pulse voltage was 800 μs in this experiment. However, the jet ended no later than 600 μs, as shown in figure 17. This behavior is different from when a pulse voltage with zero falling time is used, where a stable pulsating jet occurs when the pulse voltage is completed.

The range for pulse parameters for a stable jet might differ according to the ink properties, nozzle diameter, stand-off distance (between the head nozzle and the substrate) and the fluid delivery systems. However, the effects of pulse shape on the EHD jet discussed in this study can be referenced when the optimal conditions for the EHD jet are found. These findings are based on experimental observation, and further theoretical studies might be needed to fully understand the jetting physics.

4. Drop-on-demand printing experiments

4.1. Bitmap printing

Various printing algorithms for conventional inkjet printing systems have been developed in our laboratory. In this work, our previous works are extended to EHD jet systems to print bitmap images. During the printing, the jet behavior was monitored using a CCD camera installed in the EHD jet system. Software was developed for printing bitmap images and computer-aided design (CAD) information at a desired location on a substrate. For printing tests, x and y stages (SGSP, SIGMA KOKI, JAPAN) were used, with maximum x and y strokes of 20 mm and 85 mm, respectively. The positions of the stages are controlled by computer serial communication. A video is available online for details [14].

For drop-on-demand patterning EHD jets from each pulse voltage should repeat the same behavior. Single voltage pulses should produce single droplets, or jets equivalent to a single droplet, and the start time of jetting with respect to the pulse voltage should be consistent during the printing process.

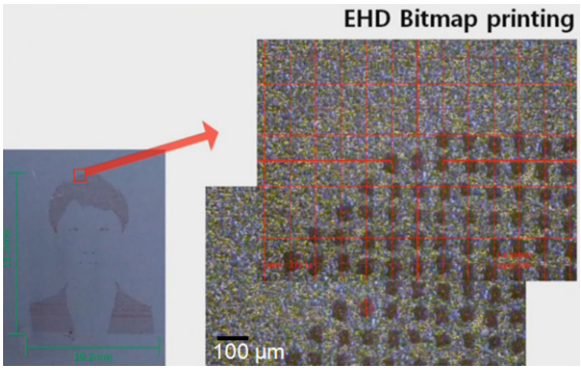

Figure 18. Drop-on-demand bitmap printing on a silicon substrate ($t_{rising} = 0$ μs, $t_{falling} = 0$ μs, $t_{dwell} = 300$ μs, $V_{pulse} = 1500$ V, $V_{dc} =$ 500 V, inner diameter of nozzle = 50 μm).

Figure 18 shows the printed results, which demonstrate that a single trigger pulse can produce a consistent pulsating jet (or equivalent single droplet). Model fluid for inkjet printing (XL-30, Dimatix, USA) was used for printing on a silicon substrate. Using a nozzle with an inner diameter of 50 μm, the printed dot size on the silicon substrate was about 30–40 μm. The size of a printed dot is related to the wettability of the substrate and the droplet amount of the pulsating jet.

4.2. Conductive ink patterning

Nano silver ink (IJ-060, Inktec, Korea) was used for printing fine, uniform conductive lines on a glass slide. To achieve conductive lines, the droplet intervals were adjusted by changing the jet frequency with fixed printing speed. The nozzle diameter should also be as small as possible to minimize the width. A nozzle with an inner diameter of 15 μm was used for printing. With a smaller-diameter nozzle, the jet behavior was difficult to observe with the CCD camera due to the optical resolution of the camera system.

Since we used different ink and a different nozzle size, the jet conditions could differ from when using standard ink. Voltage amplitudes of $V_{pulse} = 550$ V and $V_{dc} = 350$ V are used. The rising, dwell and falling times for the pulse were set to $t_{rising} = 100$ μs, $t_{dwell} = 300$ μs and $t_{falling} = 0$ μs, respectively. Figure 19(a) shows the printing results, when the stage was moved at 1 mm s^{-1} with a jet frequency of 50 Hz, so that droplets could be placed intervals of about 20 μm. As shown in figure 19(a), the droplet intervals were placed uniformly on the glass substrate.

To form a conductive line on glass substrate, the drop spacing is reduced to 10 μm by increasing the jet frequency to 100 Hz. As a result, the droplets merged to form a fine line, and a fine conductive line with a width of 15 μm could be obtained, as shown in figure 19(b). The width of conductive lines and the size of droplets could be further reduced if a nozzle with smaller diameter is used.

Figure 19(c) demonstrates the drop-on-demand patterning capability using the nano silver ink. The size of a droplet was less than 15 μm, and the distance between the droplets was set to about 30 μm. Here, the size of the droplets may differ slightly according to the jet frequency as discussed in the previous section.

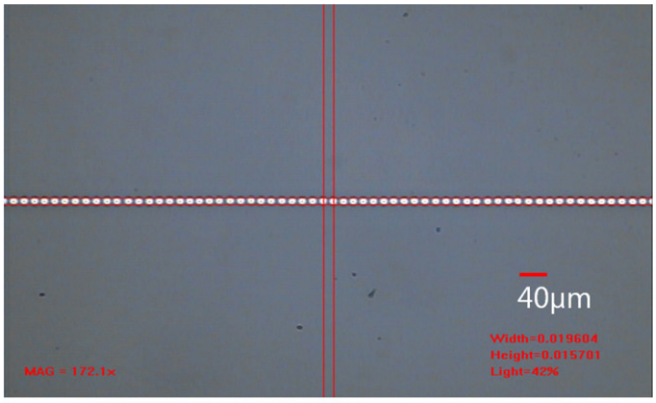

(*a*)

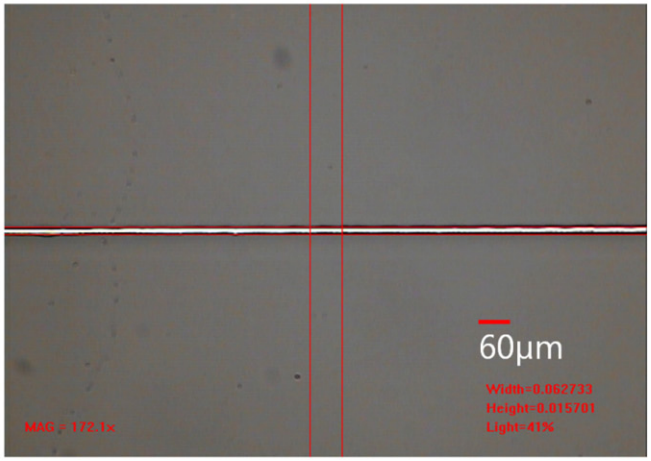

(*b*)

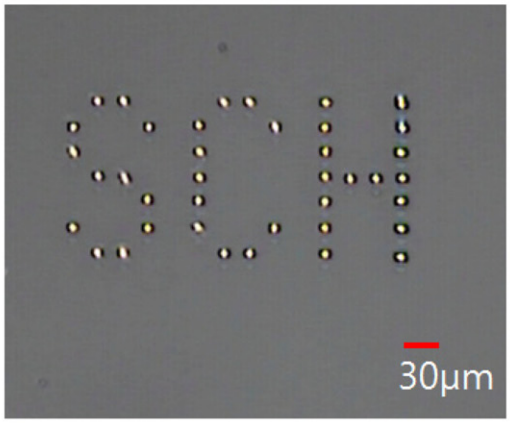

(*c*)

Figure 19. Conductive ink printing on glass substrate. (*a*) Patterning with drop spacing of 20 μm. (*b*) Printing of a conductive line (drop interval of 10 μm). (*c*) Drop-on-demand printing of SCH.

5. Conclusions

We have presented a vision measurement technique for EHD jets, and investigated how the jets are affected by the pulse voltage shape. To obtain jetting images, a CCD camera with LED strobe illumination was used. Using the sequential images acquired with this system, the meniscus behavior was analyzed with respect to time to understand the EHD jet behavior. The main features of our vision measurement are as follows: (1) the meniscus height and velocity are automatically measured and analyzed to characterize the EHD jet behavior with respect to time, and (2) the meniscus profile is extracted from each sequential image, and the meniscus profiles can be represented in a 3D graph to understand the entire EHD jet formation process.

The effects of pulse voltage on EHD jets were investigated using the measured jet behavior. In previous works, it was believed that the product of the pulse voltage amplitude and width determine the EHD jet behavior. However, in this study, it was found that the EHD jet was also affected by the pulse shape. The voltage shape effect on EHD jets can be summarized as follows:

(1) The falling part of the pulsed voltage is important because a stable pulsating jet starts after this part is applied at either the nozzle or the substrate. The amount (or duration) of the jet can be adjusted slightly by the length of the falling time. However, zero falling time is recommended for drop-on-demand printing applications to produce a consistent pulsating jet for each jet trigger signal.

(2) The rising part of the pulse voltage accounts for the initial meniscus deformation. The use of rising time results in a gradual increase in the meniscus height. However, the use of a long rising time should be avoided, since the total time for the pulse voltage can increase. The total time for the pulse voltage should be minimized to increase the jet frequency.

(3) If the dwell time, t_{dwell}, is too short, there will be no jetting. However, if t_{dwell} is too long, then there will be inconsistent dripping of ink rather than stable pulsating jets. There is a range of t_{dwell} values for stable jets. Both the rising and dwell parts of the pulse voltage have similar effects, because they are related to the initial meniscus deformation as well as the jet start time. However, the use of t_{dwell} rather than t_{rising} is effective, because the time required for initial meniscus deformation can be shortened. As a result, the maximum jet frequency can be increased. However, if the jet frequency increases, the equivalent dc voltage is affected. A high equivalent dc voltage often results in irregular dripping and a higher meniscus height prior to a jet.

To demonstrate drop consistency for drop-on-demand printing, printing results were presented, from which it was verified that consistent single pulsating jets were generated for each trigger signal under various printing conditions. The conclusions of pulse effects on jetting are based on our experimental results using ink with low viscosity (less than 20 cP). Further studies might be needed for ink with viscosity higher than 100 cP used for EHD printing.

Acknowledgments

This research was supporte by the Basic Science Research Program through the National Research Foundation of Korea (NRF), funded by the Ministry of Education, Science and Technology (2010-0021127, 2012-0007514).

References

[1] Murata K 2003 Super-fine ink-jet printing for nanotechnology *Proc. Int. Conf. on MEMS, NANO and Smart Systems* pp 346–9

[2] Park J U *et al* 2007 High resolution electrohydrodynamic jet printing *Nat. Mater.* **6** 782–9

[3] Yogi O, Kawakami T, Yamauchi M, Ye J Y and Ishikawa M 2001 On-demand droplet spotter for preparing pico- to femtoliter droplets on surfaces *Anal. Chem.* **73** 1896–902

[4] Jaworek A and Krupa A 1999 Classification of modes of EHD spraying *J. Aerosol Sci.* **30** 873–93

[5] Kim J, Oh H and Kim S S 2008 Electrohydrodynamic drop-on-demand patterning in pulsed cone-jet mode at various frequencies *J. Aerosol Sci.* **39** 819–25

[6] Mishra S, Barton K L, Alleyne A G, Ferreira P M and Rogers J A 2010 High-speed and drop-on-demand printing with a pulsed electrohydrodynamic jet *J. Micromech. Microeng.* **20** 095026

[7] Li J and Zhang P 2009 Formation and droplet size of EHD dripping induced by superimposing and electric pulse to background voltage *J. Electrost.* **67** 562–7

[8] Li J L 2006 On the meniscus deformation when the pulsed voltage is applied *J. Electrost.* **64** 44–52

[9] Podlinski J, Kocik M and Mizeraczyk J 2008 Measurements of ED flow patterns in ESP with DC+Pulsed voltage hybrid power supply *J. Phys.: Conf. Ser.* **142** 012037

[10] Choi H K, Park J U, Park O O, Ferreira P M, Gerogiadis J G and Rogers J A 2008 Scaling laws for jet pulsations associated with high-resolution electrohydrodynamic printing *Appl. Phys. Lett.* **92** 123109

[11] Lee M W, Kang D K, Kim N Y, Kim H Y, James S C and Yoon S S 2012 A study of ejection modes for pulsed-DC electrohydrodynamic inkjet printing *J. Aerosol Sci.* **42** 1–6

[12] Lee S, Song J and Chung J 2011 Drop on demand electrohydrodynamic printing induced by square pulse voltage signal *Proc. KSME Fall Spring Conf.* pp 2907–11

[13] Kwon K S 2009 Waveform design methods for piezo inkjet dispensers based on measured meniscus motion IEEE/ASME *J. Microelectromech. Syst.* **18** 1118–25

[14] Kwon K S 2012 www.youtube.com/watch?v=R71Xxbw6NzU